[CANCER RESEARCH 64, 2371–2381, April 1, 2004]

Chromatin Assembly Factor-1, a Marker of Clinical Value to Distinguish Quiescent from Proliferating Cells

Sophie E. Polo,[1] Stamatios E. Theocharis,[2] Jerzy Klijanienko,[2] Alexia Savignoni,[3] Bernard Asselain,[3] Philippe Vielh,[2] and Geneviève Almouzni[1]

Laboratories of [1]Nuclear Dynamics and Genome Plasticity, [2]Pathology, and [3]Biostatistics, Curie Institute/CNRS, Paris, France

ABSTRACT

Histone synthesis and chromatin assembly are mainly associated with DNA replication and are thus intimately involved in cell cycle regulation. The expression of key components involved in these events in human cells was studied in relation to cell-proliferative status. Among several chromatin assembly factors, chromatin assembly factor (CAF)-1 stood out as the most discriminating marker of the proliferative state. We show, using both immunofluorescence and Western blot analysis, that the expression of both CAF-1 large subunits, p150 and p60, is massively down-regulated during quiescence in several cell lines. Upon exit from the quiescent state, the CAF-1 subunits are re-expressed early, before DNA replication. The amounts of either total or chromatin-associated pools of CAF-1 proteins correlate directly with cell proliferation. Regulation of CAF-1 expression is partly controlled at the RNA level, as shown by quantitative reverse transcription-PCR and Northern blot experiments. Biological material from benign and malignant human breast tumors analyzed by immunocytochemistry and immunohistochemistry exhibits a strong positive correlation between CAF-1 p60 expression and the following proliferation markers: S-phase fraction ($r = 0.84$, $P < 0.0001$); Ki-67 ($r = 0.94$, $P < 0.0001$); and proliferating cell nuclear antigen ($r = 0.95$, $P = 0.0001$). We discuss the advantages of using CAF-1 to assess cell proliferation. High CAF-1 p60 levels are also shown to be associated with various prognostic factors. Our data highlight the precise association of CAF-1 expression with the proliferative state and validate the use of this factor as a useful proliferation marker and prognostic indicator in malignant and benign breast lesions.

INTRODUCTION

In eukaryotic cells, nuclear DNA is compacted with proteins in the form of chromatin (1). During each cell cycle, DNA must be duplicated and the chromatin structure re-established, which requires a tight coordination with histone synthesis (2). Therefore, defects affecting any of these events are likely to impinge on cell cycle progression. Histone deposition (3) is particularly interesting in this context because it depends both on the availability of histones and on the assistance of auxiliary factors, among which chaperones represent a family of proteins that have recently gained significant interest (4, 5). How these factors cooperate in histone metabolism, in a network contributing to an assembly line, is currently a matter of investigation. Histone chaperones can potentially promote nucleosome formation in various ways; (*a*) they can act directly in the histone deposition step or as histone providers, and (*b*) their nucleosome assembly activity can be coupled or not to DNA synthesis. In the present study, we have focused on the following three histone chaperones: chromatin assembly factor (CAF)-1 (6); antisilencing funtion (ASF)1 (7); and Hir-related factor (HIR)A proteins (8).

CAF-1 is best known for its ability to facilitate deposition of histones H3 and H4 on newly synthesized DNA (9). CAF-1 is a heterotrimeric complex comprising p150, p60 (6, 10), and p48 subunits (11). The p48 subunit is an escort protein that is part of several additional complexes involved in histone metabolism. We therefore chose to follow CAF-1 through its two unique and largest subunits. The direct coupling between CAF-1 activity and DNA replication highlights its critical role during S phase. In addition, expression of a dominant-negative mutant of CAF-1 p150 has been shown to lead to an S-phase arrest (12), suggesting that CAF-1 activity could be required for S-phase progression.

In the case of ASF1, two isoforms, ASF1a and ASF1b, have been identified in human cells (13). Both of them can interact with CAF-1 p60, and ASF1 proteins can synergize with CAF-1 in chromatin assembly coupled to DNA synthesis (14). In addition, a potential link with cell cycle regulation, mainly through the checkpoint kinases of the ataxia telangiectasia-mutated family, has been proposed (15).

Finally, HIRA, a single polypeptide in humans (16) can regulate histone gene expression (17) and act in a chromatin assembly pathway independent from DNA synthesis (18). Interestingly, overexpression of HIRA also leads to cell cycle defects (17).

To gain insights into how these assembly factors are controlled and whether they may represent physiologically relevant targets for cell cycle regulation, of interest for human health, we decided to examine their expression as a function of cellular proliferation in both cultured cells and clinical samples. Specifically, our aim was to analyze differences between proliferating and quiescent cells.

We show that both CAF-1 subunits are massively down-regulated in quiescent cells compared with cycling populations, whereas the expression of the chromatin assembly factor HIRA remains constant. On the other hand, the CAF-1 partner ASF1 displays a more complex pattern of regulation. Because CAF-1 subunits were found to be good indicators of the proliferative state, their expression was analyzed further. Following exit from the quiescent state, CAF-1 subunits were detected early after cell cycle entry, before S phase. We also distinguished the total pool of CAF-1 from the fraction tightly associated with chromatin, which is believed to correspond to the active molecules (19). The amount of CAF-1 proteins corresponding to each pool correlated directly with the proliferative state of the cells. This result supports a connection between the regulation of the amount of available CAF-1 in a cell and its usage at the chromatin level. Furthermore, we found that CAF-1 expression appeared to be regulated largely at the RNA level, when comparisons were made based on the proliferative state. These data encouraged us to examine CAF-1 status under various physiological conditions in human samples and more specifically in the context of cancer pathology. Tumor cells are generally characterized by a deregulated high rate of proliferation (20), and the proliferation rate of a tumor is often related to the clinical prognosis.

Received 9/18/03; revised 12/16/03; accepted 2/03/04.

Grant support: A fellowship from a collaborative program between the Curie Institute and the Commissariat à l'Energie Atomique (PIC Paramètres Epigénétiques) supported this work. S. E. Theocharis was also supported by this fellowship, by UICC (International Union Against Cancer), and by Euratom (FIGH-CT1999-00010) grants. UMR 218 was supported by la Ligue Nationale contre le Cancer (Equipe labelisée la Ligue), Euratom (FIGH-CT1999-00010), and the Commissariat à l'Energie Atomique (LRC no. 26).

The costs of publication of this article were defrayed in part by the payment of page charges. This article must therefore be hereby marked *advertisement* in accordance with 18 U.S.C. Section 1734 solely to indicate this fact.

Note: The present address for S. E. Theocharis is the Department of Forensic Medicine and Toxicology, Medical School, University of Athens, 75, Mikras Asias Street, GR 11527, Athens, Greece. Supplemental data for this article can be found at Cancer Research Online (http://cancerres@aacrjournals.org).

Requests for reprints: Geneviève Almouzni, Laboratoire de Dynamique Nucléaire et Plasticité du Génome, UMR 218, Institut Curie/CNRS, 26, rue d'Ulm, 75248 Paris cedex 5, France. Phone: 33-142-34-6701; Fax: 33-146-33-3016; E-mail: Genevieve.Almouzni@curie.fr.

Proliferation rate can be estimated in the following two ways (21): (*a*) by detecting cells at one of the phases critical for cell proliferation such as mitosis (mitotic index) or replication (S-phase fraction) or alternatively (*b*) through the presence of proliferation-associated proteins. Examples of the latter include proliferating cell nuclear antigen (PCNA; Ref. 22, 23), Ki-67 (24, 25), and the minichromosome maintenance (MCM) proteins, whose use as proliferation markers has recently been revealed (26–28). The properties of CAF-1 discovered in this study rendered it a reasonable candidate for comparison with representative markers of the two types described above. We have therefore evaluated CAF-1 as a marker of clinical value.

MATERIALS AND METHODS

Cell Culture, Synchronization. HeLa cells (gift from M. Bornens, Paris, France); MCF7, T47D, and Hs578T mammary tumoral cells (gift from O. Delattre, Paris, France); Hs578Bst mammary normal cells (LGC Promochem, Molsheim, France); and 1BR3 skin primary fibroblasts (gift from D. Papadopoulo, Paris, France) were grown in Petri dishes (Falcon Plastics, Cockeysville, MD) in the appropriate medium complemented with 10% FCS, 10 mg/ml antibiotics (penicillin and streptomycin), and 2 mM L-glutamin (Invitrogen, Carlsbad, CA). HeLa and MCF7 cells were grown in DMEM, T47D cells were grown in RPMI, Hs578T cells were grown in RPMI complemented with 10 mg/ml insulin (Invitrogen), Hs578Bst cells were grown in DMEM complemented with 30 ng/ml epidermal growth factor (PeproTech, Rocky Hill, NJ), and 1BR3 cells were grown in MEM. Normal Hs578Bst cell line is derived from the same patient as Hs578T tumoral cell line.

HeLa cells were synchronized in G_1, S, and G_2 by a double thymidine block, as follows: 25-h block in 2 mM thymidine (Sigma-Aldrich, Lyon, France); 12-h release in 30 μM 2′-deoxycytidine (Sigma-Aldrich), 25-h block in 2 mM thymidine followed by 3-, 8-, and 14-h release in 30 μM 2′-deoxycytidine to collect S, G_2, and G_1 cells, respectively. HeLa mitotic cells were obtained by mitotic shake-off after 19 h of treatment with 10 ng/ml nocodazole (Sigma-Aldrich). 1BR3 cells were blocked in G_0 by 4 days of serum starvation, and MCF7 cells were blocked in G_0 by 48 h of treatment with 10 nM ICI182780, an estrogen receptor antagonist (Fischer Bioblock Scientific, Ilkirch, France; Ref. 29). 1BR3 cells were released from G_0 by adding serum in culture medium, and MCF7 cells were released from G_0 by treatment with 100 nM 17-βestradiol E2 (Sigma-Aldrich; Ref. 30). Synchronization analyses were performed by flow cytometry after propidium iodide intercalation (Sigma-Aldrich). Percentages of replicating S-phase cells were determined by flow cytometry after BrdUrd incorporation (Sigma-Aldrich).

Antibodies. Primary antibodies used were anti-p150 mAb7655 and anti-p60 mAb8133 (Abcam, Cambridge, United Kingdom), anti-p60 poly (gift from T. Krude), anti-ASF1 obtained using recombinant proteins produced at our laboratory (immunization from Agrobio, Villeny, France), antiheterochromatin protein 1α 2G9 (Euromedex, Mundolsheim, France), anti-HIRA (gift from P. Adams), anti-Ki67 MIB1 (Dako, Carpinteria, CA), anti-PCNA PC10 (Dako), anti-MCM2 BM28 (BD PharMingen, San Diego, CA), anti-BrdUrd (Harlan Sera-Lab, Loughborough, United Kingdom), anti-cdc6 sc-8341 (Santa Cruz Biotechnology, Santa Cruz, CA), and anti-βactin AC15 (Sigma-Aldrich). Anti-p60 mAb8133 only recognizes the phosphorylated forms of p60 whereas anti-p60 poly recognizes both phosphorylated and unphosphorylated forms. Secondary antibodies coupled to FITC or Texas red were purchased from Jackson ImmunoResearch Laboratories (West Grove, PA).

Immunofluorescence. Immunofluorescence on paraformaldehyde-fixed cells was performed as described previously (19) using an epifluorescence microscope (model DMRHC; Leica, Deerfield, IL) equipped with a HBO100 mercury lamp (Osram, München, Germany), a CoolSnap FX camera (Roper Scientific, Duluth, GA) and Metamorph 4.6 software (Universal Imaging Co., Marlow, Buckinghamshire, United Kingdom) for image acquisition. Images were processed using Adobe Photoshop 5.5 software (San Jose, CA). The percentages of positively stained cells were obtained by counting at least 500 cells in each case. BrdUrd immunodetection was performed as described previously (31).

Cell Extracts, Western Blot. Nuclear, cytosolic, total, and Triton cell extracts were prepared and subjected to Western blotting as described previously (19). Serial dilutions were loaded for each sample to check signal linearity. Protein amounts were estimated by Bradford analysis (for nuclear and cytosolic extracts), by detection of βactin levels (for total extracts), or by Ponceau staining (for Triton cell extracts). Quantification was performed using Quantity One 4.2.1 software.

RNA Extracts, Real-Time Quantitative RT-PCR, Northern Blot. Total RNA was extracted using RNA NOW (Biogentex, Seabrook, TX) according to the manufacturer's instructions. To avoid any contamination by genomic DNA, DNA was digested by DNase1 Rnase-free RQ1 (Promega, Madison, WI) for 30 min at 37°C. DNase 1 was then inactivated by heating at 65°C for 10 min.

A quantification of *p150* and *p60* RNA levels was performed relative to *βactin* RNA level as an internal control. The following primer pairs (Sigma Genosys, Cambridge, United Kingdom) were designed using Oligo6 software: p60-forward, CGGACACTCCACCAAGTTCT; p60-reverse, CCAGGCGTCTCTGACTGAAT; p150-forward, GGAGCAGGACAGTTGGAGTG; p150-reverse, GACGAATGGCTGAGTACAGA; βactin-forward, ACCCCGTGCTGCTGACCGA; βactin-reverse, GCACAGCCTGGATAGCAAC. Total RNA extracts were used in independent RT reactions with the Omniscript RT kit (Qiagen, Santa Clarita, CA) using the corresponding reverse primers except for p150 RT in Hs578Bst cell line requiring another reverse primer (GGCACAAAGAAACCATCGTC) to increase amplification specificity. Quantitative amplifications were performed with the LightCycler Fast Start DNA Master SYBR Green I kit (Roche Diagnostics, Basel, Switzerland) according to the manufacturer's instructions during 45 cycles at a hybridization temperature of 60°C. Amplification efficiency was determined from serial 1:5 dilutions of the RT products. Considering every amplification 100% efficient, the relative amount of *p150* or *p60* RNA normalized to the internal control *βactin* was calculated as follows:

$$2^{-\Delta\Delta C_T} \text{ where } \Delta\Delta C_T = (C_{T\,\text{target}} - C_{T\,\text{actin}})_{\text{sample}} - (C_{T\,\text{target}} - C_{T\,\text{actin}})_{\text{calibrator}},$$

the target is *p150* or *p60*, and the calibrator is arbitrarily chosen as asynchronous MCF7 cells. Fifteen μg of each RNA sample were subjected to a Northern blot analysis according to Sambrook *et al.* (32) with the following modifications. RNA was transferred overnight to Hybond *N* + membrane (Amersham Biosciences, Orsay, France) before UV cross-linking. Membrane hybridization was performed overnight at 60°C in Rapid Hyb Buffer (Amersham Biosciences) containing the DNA probe. Human *βactin* cDNA control probe (1.8 kb) was purchased from BD Clontech (San Jose, CA); *p150* and *p60* cDNA probes (1.2 kb each) were obtained by double digestion of plasmids containing the corresponding full-length cDNA (10) and purification of the digestion product from an agarose gel. Random probe labeling was carried out using Rediprime II kit (Amersham Biosciences) with [α-^{32}P]dCTP (50μCi/25 ng of DNA probe) according to the manufacturer's instructions. Detection was achieved using PhosphorImager STORM 860 (Molecular Dynamics, Sunnyvale, CA).

Patients and Specimens. One hundred breast tumoral samples obtained from 98 patients were included in this study. Before diagnostic investigations, each patient gave informed consent. The age of the patients ranged from 18 to 98 years (mean, 56.8 years). Tumors were nonpalpable (T_0) in 8%, T_1 in 17%, T_2 in 49%, and T_3 and T_4 in 26% of cases. Sixty-four patients were node negative, and 34 had palpable axillary lymphadenopathies. Fine needle aspirations were performed by a pathologist during a specialized consultation at the Institut Curie (Paris, France). Nonpalpable tumors were sampled using ultrasound-guided technique. Aspirates were smeared on two slides for diagnosis and on three other slides (Superfrost +) for immunocytochemical studies. Histologically, eight tumors proved to be benign (fibroadenomas, 5; abscess, 2; tuberculoid granuloma, 1), and 92 tumors proved to be malignant. Among malignancies, 1 was ductal *in situ*, 79 ductal infiltrative, 8 lobular infiltrative, and 4 belonged to other types of infiltrative malignancies. Carcinomas were graded as I in 13, II in 45, and III in 31 cases. Eleven cases were nongradable. Status of estrogen receptors was determined by immunohistochemistry on histological sections in 90 cases presenting positivity in 64 cases whereas 26 were negative.

DNA Flow Cytometry. All DNA flow cytometry analyses were performed on a FACScan flow cytometer (Becton Dickinson, San Jose, CA) equipped with a doublet discrimination module. Nuclear DNA content was measured by flow cytometry on cell suspensions obtained by fine needle aspiration. Clinical samples were checked before analysis by light microscopy on cytocentrifuged

preparations stained using the May-Grünwald-Giemsa procedure to verify that at least 80% of material was composed of tumoral nuclei. Data files from at least 10,000 nuclei stained using propidium iodide were acquired in list mode. Tumors with a DNA index ranging from 0.9 to 1.1 were classified as diploid; those with a single DNA index lower than 0.9 or over 1.1 were classified as aneuploid; and the others were classified as multiploid. S-phase fractions were computed using ModFit LT 2.0 software (Verity Software House, Topsham, ME). Tumors were DNA diploid in 41 cases and DNA aneuploid/multiploid in 58 cases (in 1 case, ploidy could not be determined). S phase ranged from 0.3 to 31.4% (mean, 5.76%). S-phase percentages were subdivided into the following four groups (proliferation indexes): very low (0–2%); low (2–4.5%); moderate (4.5–10%); and high (>10%); standards commonly used for clinical studies at the Curie Institute.

Immunocytochemistry, Immunohistochemistry. Immunostainings for p60, Ki-67, and PCNA were performed on paraformaldehyde-fixed smears or on formalin-fixed paraffin-embedded tissue sections (4 μm) using the appropriate antibody, a Vectastain Elite ABC- peroxidase kit (Vector Laboratories, Peterborough, United Kingdom) and the Liquid DAB Substrate-Chromogen System (Dako) according to manufacturer's instructions. For every antigen detection in paraffin-embedded tissues and for Ki-67 detection in smears, an additional step of antigen retrieval [citrate buffer (pH 6.1) and microwave heating] was performed before antibody incubation. Cells were counterstained with hematoxylin (Merck, Darmstadt, Germany).

Statistical Analysis. The percentages of positively stained cells in immunocytochemistry experiments were obtained by counting at least 1000 cells in each case by two independent observers. Concordance between the two observers was demonstrated by calculating an intra-class correlation coefficient, allowing us to use the mean values for the after statistical analyses. Correlations were evaluated using the Spearman rank test. Average comparisons between multiple groups were determined by ANOVAs in case of homogeneous variances (according to the Bartlett test) or by the Kruskal-Wallis test. Statistical significance was taken as $P < 0.05$. Statistical analyses were performed using SPlus 2000 software.

RESULTS

In Quiescent Cells, the Expression Pattern of the Assembly Factors CAF-1, ASF1, and HIRA Revealed a Major Down-Regulation of CAF-1. First we analyzed the expression of CAF-1 p150 and p60 subunits during the cell cycle by Western blot on whole-cell extracts derived from synchronized HeLa cells. As described previously (33), variations in p60 phosphorylation profile could be detected (Fig. 1*A*). However, except in mitosis where hyperphosphorylated forms of CAF-1 may be more difficult to reveal with our antibodies, CAF-1 p150 and p60 subunits appeared to be expressed essentially in comparable amounts at all stages of the cell cycle consistent with a previous report (33). In that report, CAF-1 purified from cells throughout interphase was also shown to be competent for chromatin assembly *in vitro*. Therefore, CAF-1 expression and activity are not restricted to S phase (*i.e.*, replicating cells). A major issue then is whether CAF-1 expression is maintained or not when cells exit from the cell cycle to enter quiescence. To investigate CAF-1 expression in nonproliferating cells, we compared p150 and p60 expression levels by cellular immunodetection and semiquantitative Western blot in quiescent (G_0) and asynchronously proliferating cells. Tumoral MCF7 cells were arrested in G_0 by ICI182780 (29). Flow cytometry analysis indicated that, after treatment, BrdUrd incorporation dropped from 36% to 3% and 93% of the cells were arrested in G_0/G_1. G_0 was distinguished from G_1 by the reduced expression level of cdc6 (below the detection limits in Western blot, data not shown). We thus estimated blocking efficiency at about 93%. Immunofluorescence experiments revealed a nuclear location and colocalization of CAF-1 p150 and p60 in MCF7 cells (Fig. 1*B*) as observed previously in HeLa cells (34). The staining in these cells also displayed characteristic S-phase profiles as described previously for HeLa (31). Most importantly, a noticeable decrease in the number of cells expressing p150 and p60 was observed after G_0 block. Indeed, the numbers gave a drop from 86% to 8% (Fig. 1*B*). The proportion of cells still expressing p150 and p60 after G_0 arrest (8%) is consistent with our blocking efficiency and thus may reflect cells that have escaped synchronization.

The lack of CAF-1 detection by immunofluorescence in G_0 cells could be attributable to epitope masking or to a down-regulation in protein expression. To distinguish between these two possibilities, we examined CAF-1 protein levels by semiquantitative Western blot, with βactin as the loading control. We found that CAF-1 p150 and p60 expression is indeed down-regulated in G_0 cells (Fig. 1*C*). Both phosphorylated and unphosphorylated forms of p60 are affected in G_0 (10- and 7-fold decrease, respectively; supplementary Fig. S1).

Considering the massive down-regulation of CAF-1 in quiescent cells, we wondered if some of its interacting partners were similarly regulated and, if so, to what extent. PCNA is the first-described partner of CAF-1 p150 (35, 36). We observed that PCNA is also down-regulated in G_0, consistent with its use as a proliferation marker (22, 23), but to a lesser extent than CAF-1 (2-fold decrease; Fig. 1*C*, supplementary Fig. S1). This may be attributable to a longer half-life of PCNA because lower PCNA levels can be detected in long-term quiescent cells (23). Next we examined the expression of ASF-1, a histone H3 and H4 chaperone that interacts and synergizes with CAF-1 during replication and repair (14). We found that the expression of the ASF-1b isoform is substantially reduced in G_0 compared with asynchronous cells. The total level of ASF1a is less affected, but ASF1a is hyperphosphorylated in G_0. Indeed, the ratio of phosphorylated to unphosphorylated form shifts from 1:3 to 3:1 after G_0 arrest (Fig. 1*C*). In the case of heterochromatin protein 1α, another p150 partner (37), we found no significant difference between quiescent and cycling cells (Fig. 1*C*). Thus CAF-1 is regulated concordantly with several of its partners, but it still appears to be the most powerful marker for discrimination between proliferating and quiescent cells.

CAF-1 down-regulation in G_0 was confirmed in another type of cell line, 1BR3 primary fibroblasts (supplementary Fig. S2), showing additionally that this regulation is not specific for immortalized and transformed cell lines but represents a more general phenomenon. This is consistent with the direct coupling of CAF-1 activity and DNA replication. Because quiescent cells do not replicate, they would not need CAF-1 to fulfill this particular function. However, renewal of histones may still be needed in long-living resting cells, and other factors should thus ensure deposition of histones. One candidate for this function is the chromatin assembly factor HIRA. Indeed, it has been found to act independently from DNA synthesis *in vitro* with *Xenopus* egg extracts, in contrast to CAF-1 (18). It was thus interesting to compare HIRA expression to CAF-1 in quiescent cells. Remarkably, HIRA expression was not affected in G_0-arrested MCF7 cells (Fig. 1*D*), suggesting that HIRA could ensure stability of chromatin in quiescent cells.

Taken together, these results highlight the importance of the chromatin assembly factor CAF-1 as a major target for down-regulation in quiescent cells. It is noteworthy that the down-regulation level of the phosphorylated form of CAF-1 p60 in G_0 is of greater magnitude than that of any of the factors we have analyzed, including proliferation markers described previously, such as PCNA (2-fold decrease) and MCM2 (6-fold decrease; supplementary Fig. S1). We therefore believe that the amount of phosphorylated p60 could be a very good candidate for discriminating between cycling and resting cells.

The Amounts of Total and Chromatin Bound CAF-1 Correlate Directly with Cell Proliferation. To expand and generalize our findings, we studied the expression of CAF-1 subunits and CAF-1 partners in the following human mammary cell lines with different proliferation rates (estimated by BrdUrd incorporation): Hs578Bst

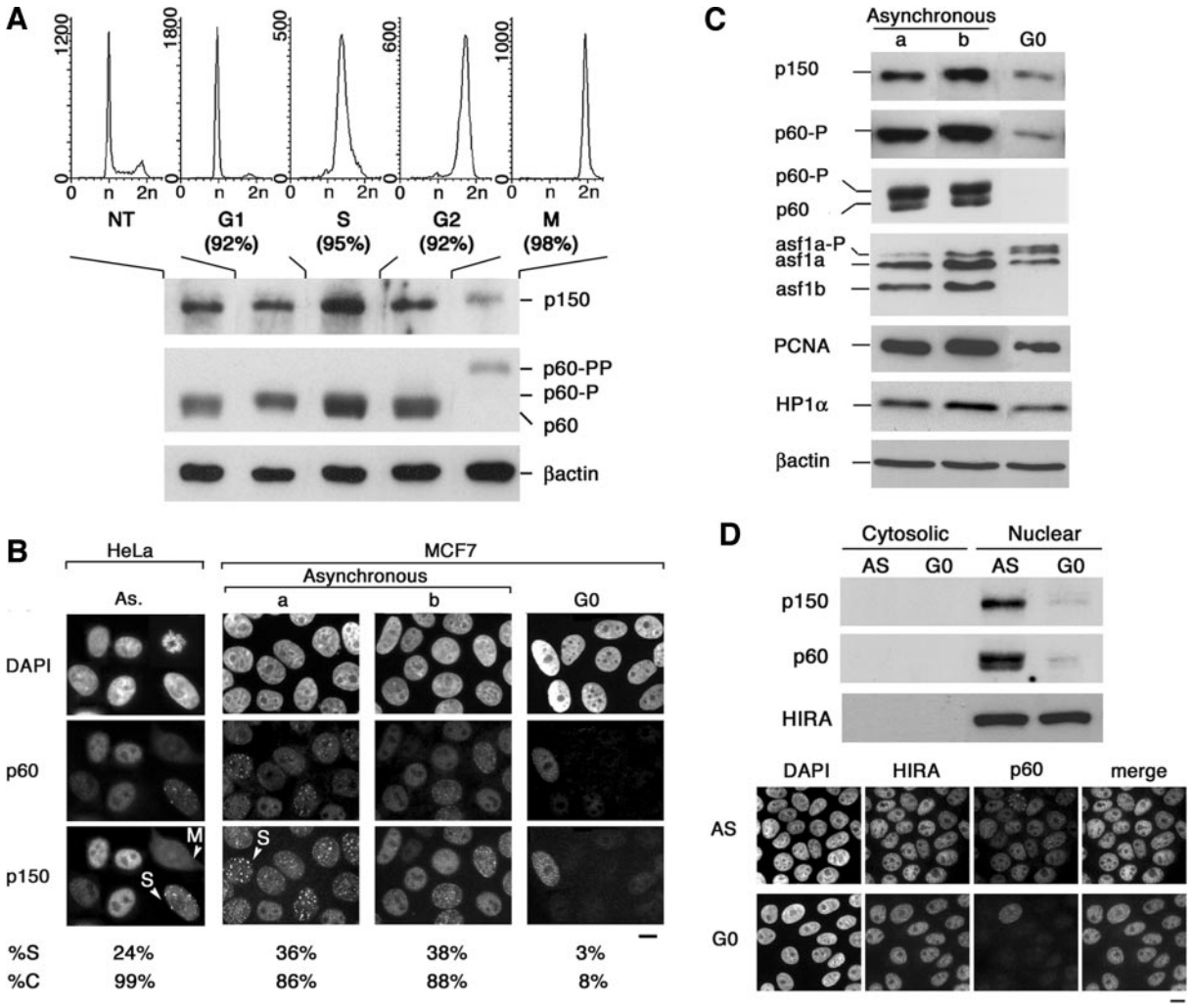

Fig. 1. G_0 regulation of chromatin assembly factor (CAF)-1 and its partners. *A*, Western blot analysis of CAF-1 p150 and p60 in total cell extracts from nontreated asynchronous (NT) and synchronized HeLa cells arrested in G_1, S, G_2 (double thymidine block), and M (nocodazole). In each case, a lysate corresponding to 10^5 cells was loaded. βactin was used as loading control. The corresponding fluorescence-activated cell sorter profiles are shown *above*. *B*, expression of CAF-1 p150 and p60 subunits revealed by immunofluorescence in asynchronous HeLa cells (As.) and in MCF7 cells. MCF7 cells are untreated (*a*), DMSO treated (*b*), or blocked in G_0 with 10 nM ICI182780 in DMSO for 48 h (G_0). S-phase fractions (%S) and percentages of CAF-1 p150 and p60 stained cells (%C) are indicated below. *Bar*, 10 μm. *C*, total cell extracts from untreated (*a*), DMSO treated (*b*), or G_0-blocked MCF7 cells were used in semiquantitative Western blot to analyze the expression of CAF-1 subunits (p150, p60) and CAF-1 partners [antisilencing funtion (ASF)1, proliferating cell nuclear antigen (PCNA), heterochromatin protein (HP)1]. For simplicity, several analyses with similar βactin levels (internal control) are juxtaposed. In each case, a lysate corresponding to 10^5 cells was loaded. *D*, *top panel*, Hir-related factor (HIR)A, CAF-1 p150, and p60 (anti-p60 poly) expression analyzed by Western blot in cytosolic and nuclear extracts from asynchronously proliferating (AS) or G_0-blocked (G_0) MCF7 cells. Ten μg of proteins were loaded in each case. *Bottom panel*, HIRA and CAF-1 p60 (anti-p60 poly) expression analyzed by immunofluorescence in asynchronous (AS) or G_0-blocked (G_0) MCF7 cells. *Bar*, 10 μm. *DAPI*, 4′,6-diamidino-2-phenylindole; *PCNA*, proliferating cell nuclear antigen; NT, nontreated.

normal cell line (13% in S phase); Hs578T (providing a comparison between cells of similar origin); and T47D and MCF7 tumoral cell lines (29, 16, and 37% in S phase, respectively). Immunofluorescence experiments (Fig. 2*A*) showed a higher percentage of cells expressing CAF-1 p150 and p60 in the tumoral cell lines (81% on average) *versus* the normal cell line (21%) and, among the tumoral cell lines, in MCF7 cells (86%) *versus* T47D cells, which proliferate more slowly (72%). Western blot experiments indicated that CAF-1 subunits (p150, p60) as well as CAF-1 partners (ASF1a, ASF1b, PCNA, and heterochromatin protein 1α) are more abundantly expressed in tumoral *versus* normal cells (Fig. 2*B*). Only a higher exposure allowed detection of the signal in normal cells. Estimation of the relative levels of CAF-1 expression in these two cell types gave at least a 6-fold difference. Taken together, these data show that the expression of CAF-1 and its partners correlates directly with cell proliferation.

CAF-1 is present in the nucleus in soluble and chromatin-bound fractions, distinguished on the basis of their resistance to detergent extraction (19). The latter fraction, by virtue of its association with chromatin, is considered to be the CAF-1 active pool. We verified that this pool was also increased in tumoral cells as shown by Western blot analysis (Fig. 2*B*). Although in normal cells the signal was below detection limit, we could clearly see a signal for the tumoral cell lines. We thus conclude that the amount of active CAF-1 is directly related to CAF-1 total amount (*i.e.*, availability) that is itself linked to the proliferative state of the cells.

CAF-1 Level Increases after G_0 Release before S-Phase Entry. Obviously, if CAF-1 decreases in G_0, a need to produce it arises when cells re-enter the cell cycle. We therefore wished to determine when CAF-1 proteins are re-expressed after G_0 release and how this is related to cell cycle progression. MCF7 cells were thus released from the quiescent phase, and progression into the cell cycle was monitored. S-phase entry occurred 12 h after G_0 release as identified by an increase in the number of cells incorporating BrdUrd (Fig. 3*A*), consistent with previous data (30). As an additional marker of cell cycle progression into S phase, the increase in cyclin A expression after release was recorded (Fig. 3*B*). During G_0 release, we could

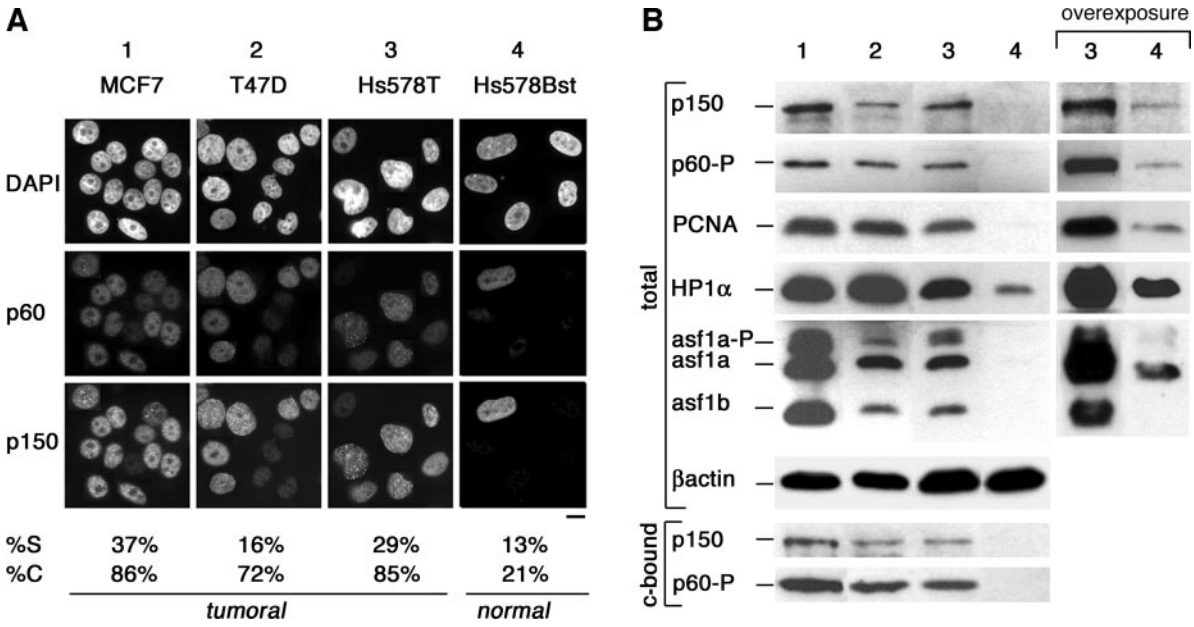

Fig. 2. Expression of chromatin assembly factor (CAF)-1 subunits and its partners in human mammary cell lines. Four human epithelial mammary cell lines were studied, as follows: three tumoral MCF7 (1), T47D (2), Hs578T (3), and one normal Hs578Bst (4). *A*, immunolocalization of CAF-1 p150 (mAb7655) and p60 (anti-p60 poly) in the indicated cell lines. Percentages of replicating cells determined by BrdUrd incorporation (%S) and percentages of CAF-1 p150- and p60-stained cells (%C) are indicated below. *Bar*, 10 μm. *B*, cell extracts from the indicated cell lines were used in semiquantitative Western blot to analyze the expression of CAF-1 subunits (p150, p60) and CAF- 1 partners [antisilencing funtion (ASF)1, proliferating cell nuclear antigen (PCNA), heterochromatin protein (HP)1]. The amount of total and chromatin-bound (c-bound) proteins is determined from total and Triton-treated cell extracts, respectively (10^5 and 25.10^4 cells/well). Western blot analyses with similar βactin levels or Ponceau staining (internal controls) are juxtaposed. An overexposure is provided to enable detection of signal in normal cells. *DAPI,* 4′,6-diamidino-2-phenylindole.

identify cells harboring distinct CAF-1-staining profiles typical of early, middle, and late S phase as described previously (31). Consistent with a progression in S phase, accumulation of late S-phase profiles was observed at the expense of early profiles as a function of time (data not shown).

The number of cells staining positively for CAF-1 p150 and p60 increased after G_0 release, as shown by immunofluorescence (Fig. 3*A*). This was confirmed semiquantitatively by Western blot analysis (Fig. 3*B*). Importantly, all S-phase cells identified by BrdUrd staining were consistently positive for CAF-1 staining, although the converse was never observed (Fig. 3*A*). Similar results were obtained after releasing 1BR3 primary fibroblasts from G_0 (supplementary Fig. S3). Although it is clear that CAF-1 p150 and p60 are re-expressed after G_0 release at an earlier time than S-phase detection by BrdUrd staining, we cannot exclude that BrdUrd staining may be less sensitive. However, immunodetection of another marker of S-phase, namely cyclin A, reinforced these previous observations. It allows us to conclude that CAF-1 subunits are re-expressed after G_0 release prior to S-phase entry, which is consistent with the CAF-1 requirement during S-phase for chromatin assembly coupled to DNA replication (38–41).

The Amount of CAF-1 RNA in a Cell Population Correlates with the Proliferative State. The regulation of CAF-1 expression linked to cell proliferation could occur at the RNA (transcription activity, RNA stability) and/or at the protein (translation activity, protein stability) level. To examine CAF-1 regulation at the RNA level, we quantified *p150* and *p60* RNA levels in comparison with *βactin* RNA level by quantitative RT-PCR (Fig. 4*A*) and Northern blot analysis (Fig. 4*B*) and obtained similar results from both experiments. The length of the amplicons from quantitative RT-PCR were as expected: 79 bp with p60 primers; 198 bp with p150 primers; and 117bp with βactin primers; amplification efficiencies were very close to each other and very close to 100%: *e.g.*, 97% for p60 primers; 99% for p150 primers; and 100% for βactin primers (data not shown). For *p60* RNA quantification, we verified that the putative transcript arising from a *p60* pseudogene on chromosome 6 was not affecting our results (supplementary Fig. S4). We found similar variations for both *p150* and *p60* RNA quantities between cell lines (Fig. 4*A*). Except for T47D cell line, in general these RNAs were less expressed in cells with low proliferation rates compared with rapidly proliferating MCF7. There was a 5-fold increase in the amount of *p150* and *p60* RNA when comparing G_0 arrested to asynchronously proliferating MCF7 cells (Fig. 4, *A* and *B*). Remarkably, this difference corresponds almost exactly to the one observed previously at the protein level (7-fold increase; supplementary Fig. S1), demonstrating that a control at the RNA level could be sufficient to account for CAF-1 expression linked to the proliferative state in this particular cell type. However, we should stress that this correspondence is not observed for Hs578T *versus* Hs578Bst cells. In this case, a higher increase was observed in protein levels (at least 6-fold; Fig. 2*B*) compared with RNA levels (about 1.5-fold; Fig. 4*A*). Interestingly, this suggests that additional regulation at the protein level can also operate in these cells, which may relate to the existence of proline-glutamic acid-serine-threonine domains in p150 and p60 subunits (10).

CAF-1 p60: A Proliferation Marker in Clinical Practice. Immunocytochemistry is routinely used for clinical purposes because this technique offers the following two major advantages in comparison with immunofluorescence: (*a*) correlation with cell morphology and (*b*) the possibility to archive slides for reassessment. We thus needed to check that our antibodies against CAF-1 could work in immunocytochemistry to assess their potential usefulness for tumor screening. Immunocytochemical staining for CAF-1 p60 was first carried out on mammary cell lines. The percentages of positively stained cells obtained by this technique (Fig. 5*A*) were consistent with our previous immunofluorescence experiments (Fig. 2*A*) but actually discriminated even more clearly between the different cell lines. The specificity of immunocytochemical detection for CAF-1 p60 was verified first by using different antibodies against p60 (monoclonal,

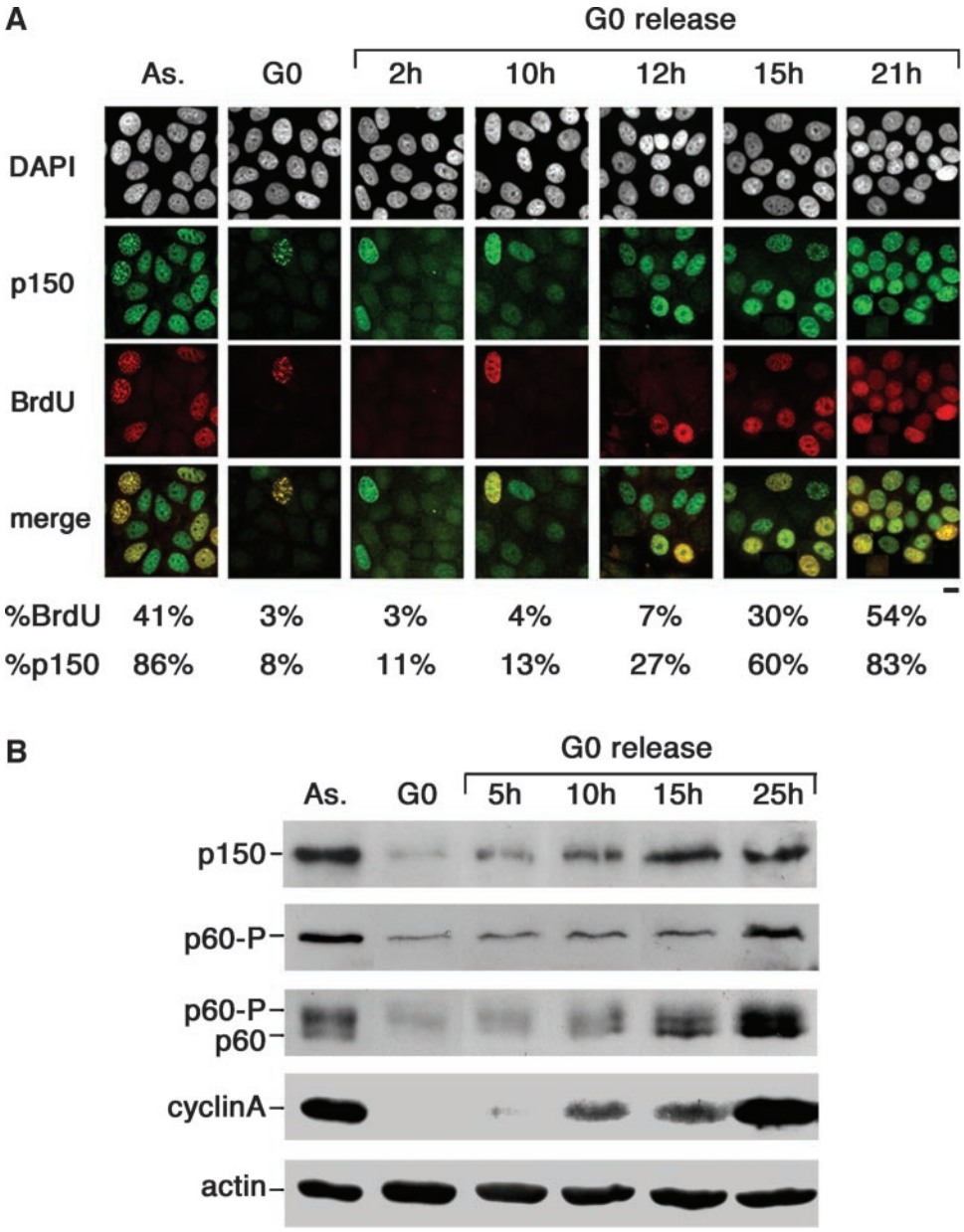

Fig. 3. Expression of chromatin assembly factor (CAF)-1 subunits after G_0 release in MCF7 cells. *A*, CAF-1 p150 expression (mAb7655) and BrdUrd incorporation analyzed by immunofluorescence in MCF7 cells at indicated times after G_0 release compared with asynchronous (As.) and G_0-arrested cells. *Bar*, 10 μm. *B*, total extracts from MCF7 cells made at indicated times after G_0 release analyzed by Western blot (10^5 cells/well) in comparison with As. and G_0-arrested cells as indicated. βactin is used as loading control, cyclin A as S-phase marker. *DAPI*, 4′,6-diamidino-2-phenylindole.

polyclonal) and second by competition with a recombinant p60 protein (supplementary Fig. S5). Consistent results were obtained when using the different sources of antibodies.

Preliminary results from immunocytochemical staining on cytology smears showed a good correlation between p60 and PCNA expression ($r = 0.95$, $P = 0.0001$) in a few cases (18; data not shown). However, because the use of PCNA as a proliferation marker has limitations attributable to antigen sensitivity to fixation time (23), we chose to pursue our analysis on a larger number of samples in comparison with the established proliferation marker Ki-67, which is widely used in routines for cancer diagnosis and prognosis (24, 25). Immunocytochemical staining of CAF-1 p60 and Ki-67 was performed on cytology smears and on paraffin-embedded tissues, showing that CAF-1 p60 antibody can be used successfully on different types of clinical material (Fig. 5, *B* and *C*). Additionally, the antibody against CAF-1 p60 allowed us to detect proliferating cells within benign breast lesions (Fig. 5, *B* and *C*). It also discriminates clearly between nontumoral and tumoral tissues, the latter showing enhanced positivity (Fig. 5*D*). In normal tissues, proliferating cells found in the basal layer of skin epithelium and in the lower third of colonic crypts (Fig. 5*E*) are positively stained with our antibody. These data prompted us to examine whether this antibody could be used as a clinical tool to mark proliferating cells.

We thus compared p60 to the Ki-67 marker by counting positively stained cells on cytology smears. The percentages obtained were concordant between two independent observers (intra-class correlation coefficient, 0.9981 for Ki-67 and 0.9983 for p60); therefore, the mean percentages were used for statistical analyses (Fig. 6). A significant correlation factor was achieved between p60 and Ki-67 expression ($r = 0.94$, $P < 10^{-4}$) showing that p60 expression is a good indicator of cell proliferation (Fig. 6*A*). The correlation level is lower with S phase, although still significant ($r = 0.83$ with Ki-67 and $r = 0.84$ with p60, $P < 10^{-4}$; Fig. 6*A*). This may be because the procedures used were different (flow cytometry *versus* immunocytochemistry) and Ki-67 and p60 are cell cycle (not only S phase) markers. Finally, we examined the correlations between CAF-1 p60 expression and several clinicopathological prognosis factors of practical use (Table 1; Fig. 6*B*). Whereas no significant association was

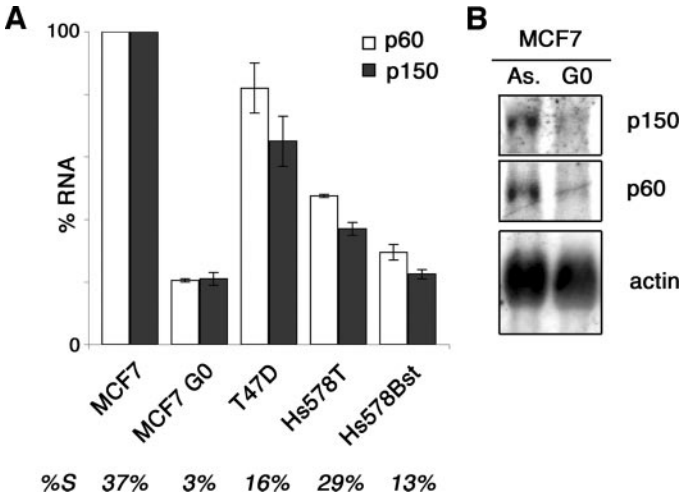

Fig. 4. Chromatin assembly factor (CAF)-1 regulation at the RNA level. *p60* and *p150* RNA levels assessed by quantitative reverse transcription-PCR (*A*) and Northern blot (*B*) relative to *βactin* RNA in total RNA extracts from mammary cell lines. *A*, graphical representation of quantitative reverse transcription-PCR results showing relative *p60* (*white*) and *p150* (*black*) RNA levels in the indicated cell lines. RNA levels are normalized to *βactin* transcripts. S-phase fractions according to BrdUrd incorporation are indicated below. *B*, Northern blot analysis of *p60* and *p150* RNA in asynchronously proliferating (As.) and G_0-arrested (G_0) MCF7 cells. The amount of *βactin* RNA was used as loading control.

noted with age and lymph node status, a clear association was found for tumor size ($P = 0.0081$), grade ($P = 0.0004$), estrogen receptor status ($P = 0.019$), proliferation index ($P < 0.0001$), and DNA ploidy ($P < 0.0001$).

These results show a strong correlation between CAF-1 detection and proliferation state in tumors on a range of clinical samples derived from breast cancer, reinforcing our conclusions drawn with cultured cells. We thus believe that CAF-1 could prove useful as a proliferation marker in clinical practice.

DISCUSSION

Our data highlight a striking correlation between CAF-1 expression and the proliferative state of cells, with a noticeable decrease in quiescent cells. This observation made in cell line models was further confirmed under physiological conditions on breast cancer samples, allowing us to propose CAF-1 as a relevant proliferation marker in this tumor type. Furthermore, we show that CAF-1 expression linked to the proliferative state is controlled mainly at the RNA level.

These results have to be considered in the light of our current knowledge of CAF-1 function. Based mainly on *in vitro* studies, CAF-1 has been shown to be involved in chromatin assembly coupled to DNA synthesis during replication (38) and repair (42). Replication is characteristic of S-phase whereas repair might occur in other phases as well as S-phase. The correlation of CAF-1 expression and cell proliferation is coherent with the S-phase function and reinforces the link with DNA replication. However, CAF-1 is also expressed outside S-phase in G_1 and G_2 (Fig. 1*A*; 19, 33), which could account for the function of CAF-1 associated with DNA repair. In the case of quiescent cells, which do not replicate DNA but in principle should also be able to undergo DNA repair, CAF-1 involvement in this process can be questioned. In this context, one can envision either that in G_0 (*a*) the low amounts of CAF-1 may still be sufficient to ensure chromatin assembly coupled to DNA repair or that alternatively (*b*) another chromatin assembly factor, yet to be identified, may substitute for CAF-1. Considering that CAF-1 promotes chromatin assembly on newly synthesized DNA, its main requirement during DNA replication would thus be associated with the elongation process. However, based on our results, it is tempting to hypothesize that CAF-1 might also be involved at the initiation step of DNA replication. Indeed, we found that CAF-1 re-expression after release from the quiescent state occurs early, before replication (Fig. 3) in parallel with MCM proteins known to be involved in the initiation of DNA replication (43).

Compared with other factors involved in chromatin assembly, CAF-1 appears as the most powerful discriminator between the proliferative and quiescent states. Indeed, contrary to CAF-1, the chromatin assembly factor HIRA is expressed at similar levels in both states (Fig. 1*D*). This strengthens previous *in vitro* results arguing that HIRA promotes chromatin assembly in a way that is independent from DNA synthesis (18). It also suggests that HIRA may be a good candidate for chromatin assembly occurring in quiescent cells that do not undergo DNA replication but still need assembly factors for histone renewal. Variations affecting ASF1 isoforms provide a more complex regulation profile as detected by Western blot (Fig. 1*C*), ASF1b being massively down-regulated compared with ASF1a, which is hyperphosphorylated. Intriguingly, this hyperphosphorylation pattern in quiescent cells is reminiscent of the pattern described in S-phase cells, resulting from Tousled-like kinase activation (13, 44). Because this hyperphosphorylation was not observed in primary cells (not shown), it may be a specific feature of tumor MCF7 cells due either to high Tousled-like kinase activity or to the involvement of additional kinases. Further investigations will be needed to clarify this complex post-translational regulation. Furthermore, we cannot distinguish between ASF1 isoforms by immunofluorescence (data not shown) compromising the use of ASF1 detection in proliferation studies by immunocytochemistry or immunohistochemistry. The data we present, showing that ASF1 isoforms do not behave in the same way, provides the first report suggestive of distinct regulatory pathways and possible functional differences between them.

We have also demonstrated that CAF-1 expression linked to the proliferative state is controlled at least in part at the RNA level (Fig. 2*B* and Fig. 4), offering a possibility to assess cell proliferation by examining CAF-1 RNA level. We should stress, however, that assessment at the protein level proved to be more reliable in all cell lines tested. Our results showing a down-regulation of CAF-1 at the RNA level in quiescent *versus* cycling cells supplement our current knowledge about the transcriptional regulation of CAF-1 during the cell cycle. Indeed, microarray analyses in human cells [HeLa cells (45, 46) and primary fibroblasts (47)] showed that CAF-1 *p150* and *p60* RNA expression is cell cycle regulated with an increase at the G_1-S boundary and a subsequent decrease in G_2-M. These variations, which are obvious in primary cells, are more difficult to observe in HeLa cells (45). In that respect, it is interesting to note that we also found it difficult to detect variations at the protein level in HeLa cells (Fig. 1*A*). This shows that observations using HeLa cells cannot necessarily be generalized and underlines the importance of taking into account the influence of the cell genetic background. In our study, the variations observed in CAF-1 expression cannot be because of widespread genetic differences as they have been observed between asynchronously proliferating and G_0-arrested cells from the same cell line (Figs. 1, *B* and *C*, and 4) and also between Hs578T and Hs578Bst lines derived from the same mammary tissue (Figs. 2 and 4). Considering the cell cycle variations of CAF-1 RNA amounts and their down-regulation after cell cycle exit, it is tempting to speculate on a possible transcriptional regulation via retinoblastoma protein/E2F. Indeed, a putative E2F binding site has been found in *p150* promoter by *in silico* studies (48). This does not exclude an additional regulation at the protein level, because CAF-1 p150 and p60 both comprise a proline-glutamic acid-serine-threonine domain (10), which is an amino acid sequence common to rapidly degraded proteins (49),

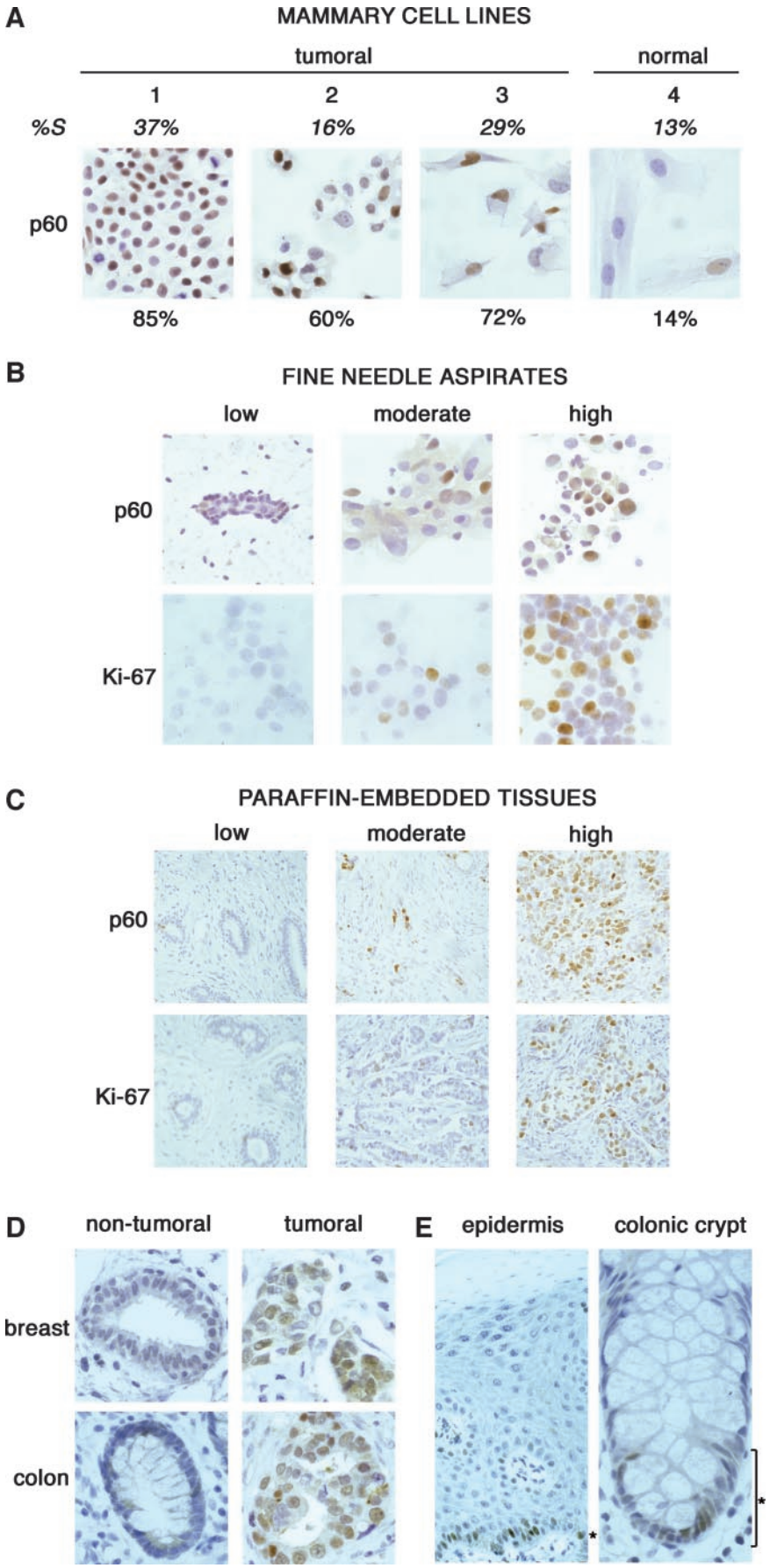

Fig. 5. Immunocytochemical and immunohistochemical detection of chromatin assembly factor (CAF)-1 p60. *A*, immunocytochemical detection of phosphorylated p60 (mAb8133) in the following four epithelial mammary cell lines: three tumoral MCF7 (1), T47D (2), Hs578T (3) and one normal Hs578Bst (4), compared with the percentage of replicating S-phase cells. Percentages of p60-stained cells obtained by counting at least 1000 cells for each cell line are indicated below. Magnification is 400×. *B*, immunocytochemical detection of Ki-67 and phosphorylated p60 (mAb8133) on fine needle aspirates from benign (low expression) and malignant breast lesions (moderate and high expression). Magnification is 400×. *C*, immunohistochemical detection of Ki-67 and phosphorylated p60 (mAb8133) in paraffin-embedded tissues from benign (low expression) and malignant breast lesions (moderate and high expression). Magnification is 200×. *D*, immunohistochemical detection of phosphorylated p60 (mAb8133) in paraffin-embedded tissues from breast and colon to compare tumoral and nontumoral tissues. Magnification is 400×. *E*, immunohistochemical detection of phosphorylated p60 (mAb8133) in paraffin-embedded tissues from normal skin (200×) and normal colon (400×). p60 expression in normal skin is restricted to the nuclei of basal and parabasal cells (*). p60 expression in normal colon is restricted to the lower third of colonic crypts (*). *%S*, percentage of cells in S-phase.

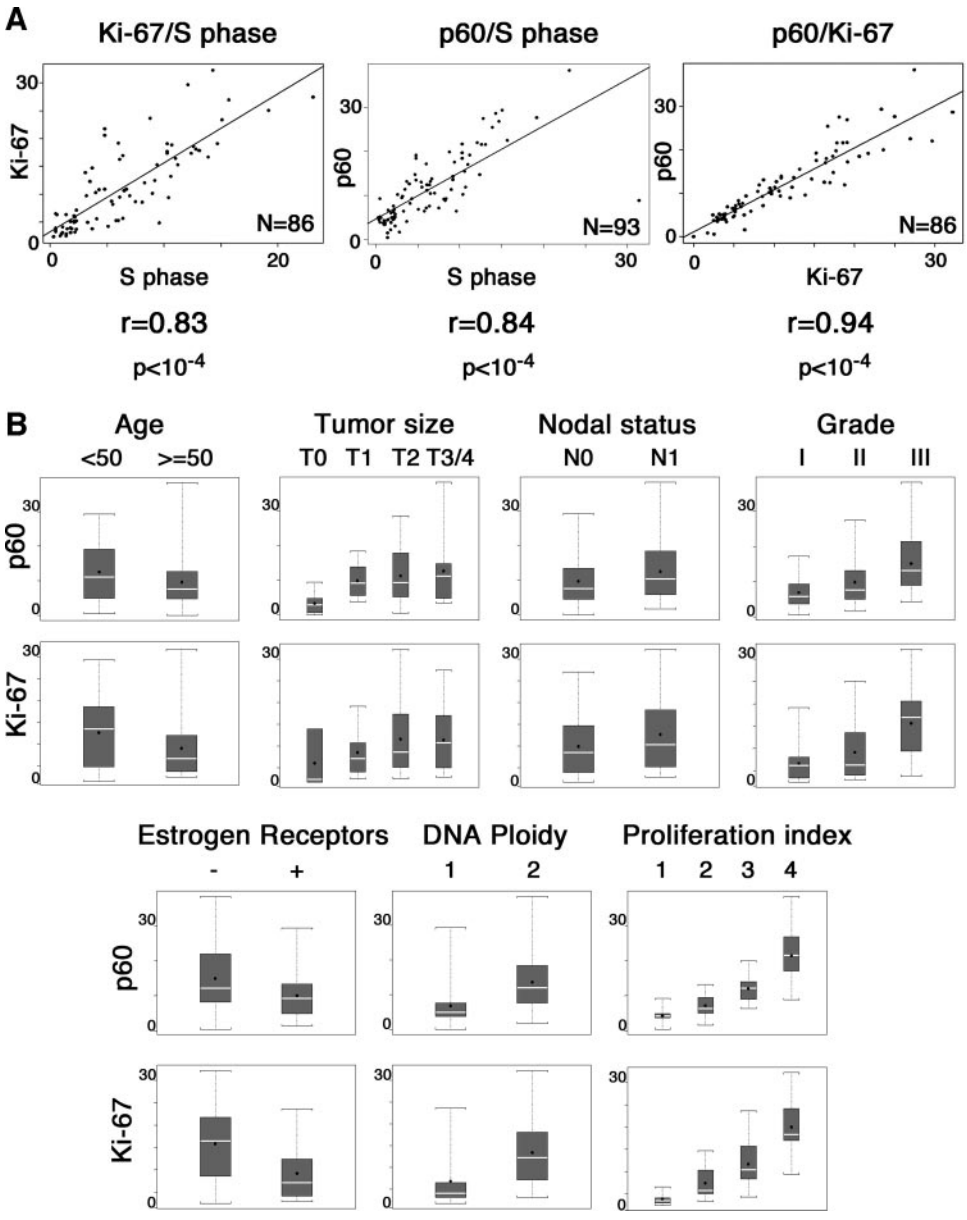

Fig. 6. Chromatin assembly factor (CAF)-1 p60, a proliferation marker in human breast cancer. All statistical analyses were done on data obtained from immunostaining on fine needle aspirates of breast tissue. *A*, graphical representation of the correlations (Spearman test) between S-phase fraction, the percentages of p60, and Ki-67 positively stained cells. *N*, number of cases; *r*, correlation factor. *B*, *boxplot* representation of p60 (*top*) and Ki-67 value distributions (*bottom*) according to the indicated prognostic factors. The *gray box* corresponds to the 25th-75th percentile. *Brackets*, range; *black point*, mean; *white line*, median. The DNA ploidy was as follows: diploid (1), aneuploid/multiploid (2). Proliferation index was as follows: very low (1), low (2), moderate (3), and high (4).

potentially acting as a signal for targeting proteins for degradation by the proteasome. Furthermore, CAF-1 activity may not be regulated only by CAF-1 protein amount but also by post-translational modifications such as phosphorylation/dephosphorylation and recruitment to DNA via PCNA as described in previous studies. Indeed, it has already been shown that CAF-1 hyperphosphorylation in mitosis inhibits its chromatin assembly activity (33) and CAF-1 phosphorylation in interphase has been associated with chromatin assembly coupled to DNA repair (19). In any case, the labeling at the protein level provides a reliable marker of cell proliferation.

Our observations in cell line models were further explored in a physiological context by studies on tissue samples. These studies showed a direct correlation at the protein level between CAF-1 p60 and several proliferation markers. This is most likely reflecting the behavior of the entire CAF-1 complex. Indeed, results from a transcriptome analysis in human breast cancer show that CAF-1 *p150* belongs to the same "proliferation cluster" as genes involved in DNA replication (50). Other proliferation markers, like PCNA (23), Ki-67 (25) and MCM proteins (28), have already been validated and used successfully in different tumoral types. However, PCNA immunoreactivity can be affected by the time of fixation (23), and the use of Ki-67 has limitations attributable to (*a*) the lack of knowledge concerning its role in cell proliferation and (*b*) the systematic requirement of an antigen retrieval step for its immunodetection. On the contrary, CAF-1 can be detected directly on cytological preparations (supplementary Fig. S6) and the link between CAF-1 and cell proliferation has been well documented, lying in a PCNA-mediated coupling between CAF-1 activity and DNA replication (35, 36). Although CAF-1 activity is also directly coupled to DNA repair (nucleotide excision repair; Ref. 42), and CAF-1 is recruited to chromatin after UV irradiation (19, 51), its expression is not induced after DNA damage (19). Thus CAF-1 detection by immunostaining is unlikely to be because of repair events and only reflects the proliferative state. Furthermore, PCNA and Ki-67 have not proved useful in every cancer type, especially for cervical smear analysis (27). On the other hand, MCM markers have only been examined in a limited number of cases in breast cancer (26), and in fact, in the normal breast, a high proportion of cells have been found to express MCM proteins (52). This suggests that the use of MCM markers may not be ideal for assessment of breast cancer. In this case, alternative markers can be

Table 1 *Average comparison of p60 and Ki-67 between multiple groups of prognostic factors*

p60 and Ki-67 values were obtained from immunocytochemistry on fine needle aspirates of breast tumors. p60 and Ki-67 average percentages are indicated for each group. Significative *P* are highlighted in bold. Proliferation indexes are classified according to the level of S-phase fraction as described in *"Materials and Methods." N*, number of cases.

	p60			Ki-67		
Clinicopathological factors	*N*	% positivity	*P*	*N*	% positivity	*P*
Age			0.062			**0.0398**
<50	39	12.49		32	12.86	
≥50	61	9.57		53	9.46	
Tumor size			**0.0081**			0.344
T_0	8	3.26		3	6.02	
T_1	17	9.79		16	8.52	
T_2	49	10.67		41	11.6	
T_3, T_4	26	12.61		25	11.32	
Nodal status			0.075			0.105
N_0	65	9.71		57	9.83	
N_1	35	12.56		28	12.6	
Grade			**0.0004**			**0.0002**
I	13	6.84		12	6.66	
II	45	9.86		40	9.14	
III	31	15.14		27	15.63	
Estrogen receptor			**0.019**			**0.002**
Negative	26	14.91		23	15.79	
Positive	64	10.03		57	9.16	
Proliferation index			**<10e-4**			**<10e-4**
Very low	23	4.3		20	3.8	
Low	21	7.2		18	7.35	
Moderate	28	12.04		24	11.62	
High	21	21.33		20	19.97	
DNA ploidy			**<10e-4**			**<10e-4**
Diploid	41	6.74		33	6.78	
Aneuploid/multiploid	58	13.51		51	13.36	

useful for following cell proliferation. Furthermore, several arguments point to the use of CAF-1 as a general marker in a variety of tumor types. In addition to the widespread conservation across species of CAF-1 (53), in humans it appears to be expressed in cells derived from a variety of tissue types [293 (38) derived from kidney, HeLa (33) derived from cervix, and 1BR3 derived from skin and mammary cells (as shown in this work)]. It will thus be of great importance to investigate further the potential use of CAF-1 p60 as a proliferation marker in many cancer types in comparison with MCM proteins. Obviously, MCM proteins do not detect only actively proliferating cells but also cells licensed for proliferation, thus they appear to be highly sensitive markers for proliferative potential (52). We propose that their use could be complemented by the use of CAF-1, which is a more specific marker of actively proliferating cells. The combined use of these two markers could provide a powerful diagnosis tool for assessing cancer progression. Additionally, long-term follow-up studies would be of major interest to determine the relationship between CAF-1 expression and patients' outcome. Finally, all proliferation markers mentioned above have been involved in DNA replication but in addition, CAF-1 provides a direct link to the control of chromatin organization that is critical for many aspects of DNA metabolism including gene expression. This may represent a good illustration of the importance of chromatin-related events in the context of cancer.

This work puts forward CAF-1 as a novel proliferation marker, potentially helpful in cancer prognosis and in monitoring tumor response to therapies. It also opens up interesting perspectives in fundamental cancer research, especially in the comprehension of how CAF-1 expression is integrated into pathways leading to tumorigenesis.

ACKNOWLEDGMENTS

We thank Danièle Rouillard and Eliane Padois for flow cytometry analyses, Véronique Mark for immunocytochemical stainings, Alexandra Rousseau for the initial statistical analyses, Danièle Roche for technical advice, Catherine Green and Edith Heard for editing the manuscript, Anja Groth and Philip Hanawalt for useful comments, and members of UMR218 for helpful discussion.

REFERENCES

1. Kornberg RD. Structure of chromatin. Annu Rev Biochem 1977;46:931–54.
2. Kaufman PD, Almouzni G. DNA replication, nucleotide excision repair, and nucleosome assembly. In: Elgin S, Workman J, editors. Frontiers in molecular biology: chromatin structure and gene expression, ed. 2. Oxford, United Kingdom: Oxford University Press; 2000. p. 24–48.
3. Mello JA, Almouzni G. The ins and outs of nucleosome assembly. Curr Opin Genet Dev 2001;11:136–41.
4. Philpott A, Krude T, Laskey RA. Nuclear chaperones. Cell Dev Biol 2000;11:7–14.
5. Loyola A, Almouzni G. Histone chaperones, a supporting role in the limelight. Biochim Biophys Acta. In press 2004.
6. Smith S, Stillman B. Purification and characterization of CAF-I, a human cell factor required for chromatin assembly during DNA replication in vitro. Cell 1989;58: 15–25.
7. Le S, Davis C, Konopka JB, Sternglanz R. Two new S-phase-specific genes from Saccharomyces cerevisiae. Yeast 1997;13:1029–42.
8. Sherwood PW, Tsang SV, Osley MA. Characterization of HIR1 and HIR2, two genes required for regulation of histone gene transcription in Saccharomyces cerevisiae. Mol Cell Biol 1993;13:28–38.
9. Ridgway P, Almouzni G. CAF-1 and the inheritance of chromatin states: at the crossroads of DNA replication and repair. J Cell Sci 2000;113:2647–58.
10. Kaufman PD, Kobayashi R, Kessler N, Stillman B. The p150 and p60 subunits of chromatin assembly factor I - a molecular link between newly synthesized histones and DNA replication. Cell 1995;81:1105–14.
11. Verreault A, Kaufman PD, Kobayashi R, Stillman B. Nucleosome assembly by a complex of CAF-1 and acetylated histones H3/H4. Cell 1996;87:95–104.
12. Ye X, Franco AA, Santos H, Nelson DM, Kaufman PD, Adams PD. Defective S phase chromatin assembly causes DNA damage, activation of the S phase checkpoint, and S phase arrest. Mol Cell 2003;11:341–51.
13. Sillje HH, Nigg EA. Identification of human Asf1 chromatin assembly factors as substrates of Tousled-like kinases. Curr Biol 2001;11:1068–73.
14. Mello JA, Sillje HH, Roche DM, Kirschner DB, Nigg EA, Almouzni G. Human Asf1 and CAF-1 interact and synergize in a repair-coupled nucleosome assembly pathway. EMBO Rep 2002;3:329–34.
15. Groth A, Lukas J, Nigg EA, et al. Human Tousled like kinases are targeted by an ATM- and Chk1-dependent DNA damage checkpoint. EMBO J 2003;22:1676–87.
16. Lamour V, Lecluse Y, Desmaze C, et al. A human homolog of the S. cerevisiae HIR1 and HIR2 transcriptional repressors cloned from the DiGeorge syndrome critical region. Hum Mol Genet 1995;4:791–9.
17. Nelson DM, Ye X, Hall C, et al. Coupling of DNA synthesis and histone synthesis in S phase independent of cyclin/cdk2 activity. Mol Cell Biol 2002;22:7459–72.
18. Ray-Gallet D, Quivy JP, Scamps C, Martini E, Lipinski M, Almouzni G. HIRA is critical for a nucleosome assembly pathway independant of DNA synthesis. Mol Cell 2002;9:1091–100.

19. Martini E, Roche DMJ, Marheineke K, Verreault A, Almouzni G. Recruitment of phosphorylated chromatin assembly factor 1 to chromatin following UV irradiation of human cells. J Cell Biol 1998;3:563–75.
20. Evan GI, Vousden KH. Proliferation, cell cycle and apoptosis in cancer. Nature (Lond) 2001;411:343–8.
21. Hall PA, Levison DA. Review: assessment of cell proliferation in histological material. J Clin Pathol 1990;43:184–92.
22. Takasaki Y, Deng JS, Tan EM. A nuclear antigen associated with cell proliferation and blast transformation. J Exp Med 1981;154:1899–909.
23. Hall PA, Levison DA, Woods AL, et al. Proliferating cell nuclear antigen (PCNA) immunolocalisation in paraffin sections: an index of cell proliferation with evidence of deregulated expression in some neoplasms. J Pathol 1990;162:285–94.
24. Gerdes J, Schwab U, Lemke H, Stein H. Production of a mouse monoclonal antibody reactive with a human nuclear antigen associated with cell proliferation. Int J Cancer 1983;31:13–20.
25. Brown DC, Gatter KC. Monoclonal antibody Ki67: its use in histopathology. Histopathology 1990;17:489–503.
26. Todorov IT, Werness BA, Wang HQ, et al. HsMCM2/BM28: a novel proliferation marker for human tumors and normal tissues. Lab Investig 1998;78:73–8.
27. Williams GH, Romanowski P, Morris LS, et al. Improved cervical smear assessment using antibodies against proteins that regulate DNA replication. Proc Natl Acad Sci USA 1998;95:14932–7.
28. Freeman A, Morris LS, Mills AD, et al. Minichromosome maintenance proteins as biological markers of dysplasia and malignancy. Clin Cancer Res 1999;5:2121–32.
29. Carroll JS, Prall OW, Musgrove EA, Sutherland RL. A pure estrogen antagonist inhibits cyclin E-Cdk2 activity in MCF-7 breast cancer cells and induces accumulation of p130–E2F4 complexes characteristic of quiescence. J Biol Chem 2000;275:38221–9.
30. Prall OW, Sarcevic B, Musgrove EA, Watts CK, Sutherland RL. Estrogen-induced activation of Cdk4 and Cdk2 during G_1-S phase progression is accompanied by increased cyclin D1 expression and decreased cyclin-dependent kinase inhibitor association with cyclin E-Cdk2. J Biol Chem 1997;272:10882–94.
31. Taddei A, Roche D, Sibarita JB, Turner BM, Almouzni G. Duplication and maintenance of heterochromatin domains. J Cell Biol 1999;147:1153–66.
32. Sambrook J, Fritsch EF, and Maniatis T. Molecular cloning: a laboratory manual, ed. 2. Cold Spring Harbor, NY: Cold Spring Harbor Laboratory Press, 1989.
33. Marheineke K, Krude T. Nucleosome assembly activity and intracellular localization of human CAF-1 changes during the cell division cycle. J Biol Chem 1998;273:15279–86.
34. Smith S, Stillman B. Immunological characterization of chromatin assembly factor I, a human cell factor required for chromatin assembly during DNA replication in vitro. J. Biol Chem 1991;266:12041–7.
35. Shibahara K, Stillman B. Replication-dependent marking of DNA by PCNA facilitates CAF-1-coupled inheritance of chromatin. Cell 1999;96:575–85.
36. Moggs JG, Grandi P, Quivy J, et al. A CAF-1/PCNA mediated chromatin assembly pathway triggered by sensing DNA damage. Mol Cell Biol 2000;20:1206–18.
37. Murzina N, Verreault A, Laue E, Stillman B. Heterochromatin dynamics in mouse cells: interaction between chromatin assembly factor 1 and HP1 proteins. Mol Cell Biol 1999;4:529–40.
38. Stillman B. Chromatin assembly during SV40 DNA replication in vitro. Cell 1986;45:555–65.
39. Kaufman PD. Nucleosome assembly: the CAF and the HAT. Curr Opin Cell Biol 1996;8:369–73.
40. Verreault A. De novo nucleosome assembly: new pieces in an old puzzle. Genes Dev 2000;14:1430–8.
41. Krude T, Keller C. Chromatin assembly during S phase: contributions from histone deposition, DNA replication and the cell division cycle. Cell Mol Life Sci 2001;58:665–72.
42. Gaillard PH, Martini EM, Kaufman PD, Stillman B, Moustacchi E, Almouzni G. Chromatin assembly coupled to DNA repair: a new role for chromatin assembly factor I. Cell 1996;86:887–96.
43. Tye BK. MCM proteins in DNA replication. Annu Rev Biochem 1999;68:649–86.
44. Sillje HH, Takahashi K, Tanaka K, Van Houwe G, Nigg EA. Mammalian homologues of the plant Tousled gene code for cell-cycle-regulated kinases with maximal activities linked to ongoing DNA replication. EMBO J 1999;18:5691–702.
45. van der Meijden CM, Lapointe DS, Luong MX, et al. Gene profiling of cell cycle progression through S-phase reveals sequential expression of genes required for DNA replication and nucleosome assembly. Cancer Res 2002;62:3233–43.
46. Whitfield ML, Sherlock G, Saldanha AJ, et al. Identification of genes periodically expressed in the human cell cycle and their expression in tumors. Mol Biol Cell 2002;13:1977–2000.
47. Cho RJ, Huang M, Campbell MJ, et al. Transcriptional regulation and function during the human cell cycle. Nature (Lond) 2001;27:48–54.
48. Elkon R, Linhart C, Sharan R, Shamir R, Shiloh Y. Genome-wide in silico identification of transcriptional regulators controlling the cell cyle in human cells. Genome Res 2003;13:773–80.
49. Rogers S, Wells R, Rechsteiner M. Amino acid sequences common to rapidly degraded proteins: the PEST hypothesis. Science (Wash D C) 1986;234:364–8.
50. Perou CM, Jeffrey SS, van de Rjin M, et al. Distinctive gene expression patterns in human mammary epithelial cells and breast cancers. Proc Natl Acad Sci USA 1999;96:9212–7.
51. Green CM, Almouzni G. Local action of the chromatin assembly factor CAF-1 at sites of nucleotide excision repair in vivo. EMBO J 2003;22:5163–74.
52. Stoeber K, Tlsty TD, Happerfield L, et al. DNA replication licensing and human cell proliferation. J Cell Sci 2001;114:2027–41.
53. Kaufman PD, Kobayashi R, Stillman B. Ultraviolet radiation sensitivity and reduction of telomeric silencing in Saccharomyces cerevisiae cells lacking chromatin assembly factor-I. Genes Dev 1997;11:345–57.